A Fluorescent Polymer for Patterning of Mesenchymal Stem Cells

Jungmok You,[†] June Seok Heo,[‡] Jiyea Lee,[†] Han-Soo Kim,[‡,§] Hyun Ok Kim,*[,‡,§] and Eunkyoung Kim*[,†]

Department of Chemical and Biomolecular Engineering, Yonsei University, Cell Therapy Center, Severance Hospital, College of Medicine, Yonsei University, and Department of Laboratory Medicine, College of Medicine, Yonsei University, 134 Shinchon-dong, Seodaemun-gu, Seoul 120-749, Korea

Received December 5, 2008; Revised Manuscript Received February 20, 2009

ABSTRACT: UV exposure of a fluorescent polymer, diphenylamino-s-triazine bridged *p*-phenylene vinylene polymer (DTOPV), resulted in fluorescence quenching and a change in surface wettability via photo-oxidation. Patterned polymer films were prepared simply by exposing the polymer film to UV source through a photomask under air. The UV-exposed region was highly biocompatible and provided selective mesenchymal stem cells (MSCs) attachment on it. This allowed cell alignment and patterning along the line patterns of linear, curved, and even various letter shapes. The proliferation rate of MSCs cultured on UV exposed surface (DTOPV+UV) was higher than that of the unexposed surface, and the cells were increased to10-fold after 6 days. The attachment of MSCs was highly selective to the UV-exposed pattern in the presence of collagen and gelatin, which induced cell patterning and attachment through hydrophilic interaction with the UV exposed area. Taking advantage of the emission from the DTOPV pattern, the cell location and pattern images were easily detected through a microscope with or without an excitation probe beam. These studies provide an exciting opportunity for novel cell patterning by a simple photopatterning process using a highly fluorescent DTOPV.

Introduction

The surface patterning of biomaterials has recently been a key technology for gene and drug delivery, and tissue engineering.[1,2] Furthermore, controlled patterning of the biomaterial enables one to tune cell attachment, proliferation, differentiation, protein secretion, etc., thereby exploring the possibilities of modern cell engineering.[2−6] The opportunity to use materials to selectively influence cell activity is based on the adhesion and selective spatial arrangement of individual cell types on a specific surface pattern of materials having preferential chemical composition,[2,7] surface charge,[8] wettability,[9] and morphology.[10] The latest studies have reported stem cell patterning to control the stem cell properties such as adhesion, growth, and differentiation.[11] The cell pattern on a specific site has been routinely identified by fluorescent labeling. Due to the high complexity and cooperative function resulting from the specific spatial organization of multiple cell types and proteins, a patternable polymer film with a label-free detection method would be beneficial for controlling biomaterial properties.

One of the biggest challenges is to pattern a biocompatible fluorescent surface in a single step to induce cell assembly directly on the pattern and detect these patterns using fluorescence microscopy. However, such experiments have been limited by low fluorescence and difficulty in patterning of the polymeric fluorescent film.

We embarked on a highly fluorescent, biocompatible, and patternable polymer film that allows micropatterning of cells with easy detection. For this purpose, a fluorescent polymer having vinylene C═C bonds was photopatterned to give dark micropatterned lines. The single step of photopatterning does not require wet etching or a deposition process. As the pattern is fluorescent, it can be examined through a fluorescent mocroscope. Furthermore, the location of the cells or biomaterials can be easily detected, without the need for labeling cells, when cells are selectively adhere and align on either fluorescent or nonfluorescent region of the polymer pattern.

In this study, we report for the first time the adhesion and patterning of mesenchymal stem cells (MSCs) on micro polymer patterns, which are formed by photo-oxidation of an s-triazine bridged *p*-phenylene vinylene polymer.[12] In addition, we discuss cell on biomedical devices is a fundamental factor for the integration process of a biomaterial after implantation.

Experimental Section

Materials. S-triazine bridged *p*-phenylenevinylene polymer (DTOPV) was synthesized through the Wittig polycondensation as reported before.[12] Weight average molecular weight (M_w) of the polymer was 6500. Crystal violet lactone (CVL) was purchased from Aldrich. α-Minimum essential medium (α-MEM), fetal bovine serum (FBS), antibiotics (penicillin/streptomycin), phosphate-buffered saline (PBS, pH 7.4), trypsin/EDTA (0.05%), and Tryphan blue (0.4%) were purchased from Gibco (Invitrogen, USA). Albumin (5%) was purchased from Green Cross Corporation (Korea). Collagen type I was purchased from BD Bioscience. Human IgG, gelatin from porcine skin type A, and fibronectin from human plasma were purchased from Sigma-Aldrich. Bone marrow (BM) derived mesenchymal stem cells (MSCs), on patient compliance, were used for this study. A frozen stock of MSCs was provided by Cell Therapy Center, Severance Hospital (from University of Yonsei, Seoul, Korea) at passage 3. Other chemicals and solvents were purchased from Aldrich.

Instruments. FT-IR spectra were obtained from a Bio-Rad Digilab Division FTS-80. The average molecular weight of the polymer was characterized by a gel permeation chromatography (GPC) (model: Waters R-401 ALC/GPC) with THF as an eluent and polystyrene standard for calibration. Fluorescence spectra were obtained with a luminescence spectrometer (PerkinElmer, Model LS55) under excitation at 370 nm The thickness of the polymer film was determined via an Alpha step profilometer (Tencor Instruments, Alpha-step IQ) with an accuracy of 1 nm. The polymer films were illuminated with a UV lamp (Rolence Enterprise, Inc., Taiwan, power: 13.05 mW/cm^2), model POWERARC UV 100. The surface wettability was investigated by a water (DI) drop contact angle measurement using contact angle meter-CAM 101 model

* Corresponding author. E-mail: eunkim@yonsei.kr.
[†] Department of Chemical and Biomolecular Engineering, Yonsei University.
[‡] Cell Therapy Center, Severance Hospital, College of Medicine, Yonsei University.
[§] Department of Laboratory Medicine, College of Medicine, Yonsei University.

10.1021/ma802722q CCC: $40.75
Published on Web 03/20/2009

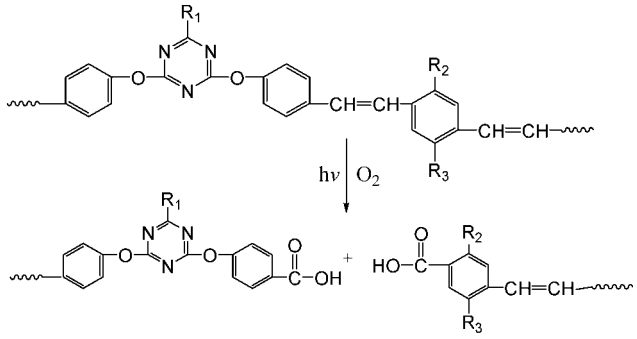

DTOPV: R_1=diphenylamino, R_2= OCH_3,
R_3 = O-$(CH_2)_2CH(CH_3)$-$(CH_2)_3$-$CH(CH_3)_2$

Figure 1. Structure and photo-oxidation reaction of DTOPV.

(KSV Instruments Ltd., Finland). Both AFM and EFM analyses were carried out at room temperature with a Dimension 3100 SPM equipped with Nanoscope IVa devised by Digital Instruments from Santa Barbara, CA. EFM tips were commercial Pt/Ir-coated Si cantilevers with force constant 2.8 N/m and they were purchased from Nanoworld (Serial No. 50091F19L392). The fluorescent patterns such as Figure 4b were imaged under Olympus-BX51 fluorescence microscope with WB-dichroic mirror DM500, excitation filter BP450-480 and barrier filter BA515. The optical MSCs patterns such as Figure 5d were obtained from Olympus inverted research microscope model IX71. Parts c−f of Figure 6 were obtained under the same optical microscope but under illumination of a blue probe beam (460−480 nm, 17.5 mW/cm^2). During the microscopic imaging, there was no change in pattern or cell attachment behavior. To detect changes of cell morphology more in detail, MSCs were observed with field emission-scanning electron microscope (HITACHI S-800, Tokyo, Japan) and the picture was taken by scanning microscope image analysis system (ESCAN-4000, Bummi Universe, Tokyo, Japan).

Preparation of DTOPV Film and DTOPV Pattern Substrates. The DTOPV films having average thickness 140 nm were prepared by spin coating with the chloroform solution of DTOPV (1 wt %) at 13 000 rpm for 15 s and then dried for solvent removal. These DTOPV films without pattern were used for the spectroscopic measurements, contact angle measurement, and the proliferation assay of MSCs. For fluorescent pattern formation, the DTOPV films were illuminated with a high-intensity UV lamp (13.05 mW/cm^2) through a photomask. These DTOPV patterns were used for the AFM, EFM study, MSCs pattern, and proteins assay.

Analyses of DTOPV Surface with Contact Angle, AFM, and EFM Measurements. Surface wettability of the DTOPV films through photo-oxidation was investigated by water (DI) drop contact angle measurement. DOTPV films were illuminated by high intensity UV source (0, 11.7, 23.4, 35.1, 46.8 J/cm^2). For surface morphology experiments, the polymer films on silicon wafer were illuminated by a high-intensity UV source (23.4 and 46.8 J/cm^2) through a 5 μm line photomask. To investigate the surface topographic and electrostatic properties simultaneously, the instrument was operated in two-pass, interleaved scanning mode. In the first pass, the surface topography was obtained from a tapping mode scan with no external voltage applied. The AFM tip was oscillated at its resonance frequency (75 kHz). Next, the tip was lifted with fixed distance above the sample surface and scanned at that constant height with a voltage applied. The tip was raised 40 nm during EFM scanning with a +9 V voltage applied. Images were obtained at scan rate of 0.6 Hz for both.

Cell Culture. MSCs were thawed, placed at a density of about 10,000 cells/cm^2 in 15 mL medium (α-MEM supplemented with 10% FBS, 100 U/mL penicillin and 100 μg/mL streptomycin) in a 75 cm flask (Nunc, Denmark), at 37 °C in 5% humidified CO_2. Medium was replaced with fresh α-MEM with 10% FBS, 100 U/mL penicillin and 100 μg/mL streptomycin every 3 or 4 days and cells were grown to 90−95% of confluence over about 3−7 days. Once the cells reached confluence, they were detached using 0.05% Trypsin/EDTA and replaced for further expansion. The MSCs in this study were between passage of 4 and 7.

Cell Attachment to Micropatterned DTOPV Substrate. For cell patterning studies, the DTOPV pattern on a glass substrate (1.6 cm × 2.8 cm) was prepared with energy dose of 23.4 J/cm^2. The micropattern substrates were placed in six well plate (Nunc, Denmark) containing culture medium, α-MEM supplemented with 10% FBS, 100 U/mL penicillin and 100 ug/mL streptomycin. MSCs were detached from cell culture substrates by trypsinization. The cells at a concentration of 4,000 cells/cm^2 were seeded on a patterned substrate in six well plate (Nunc, Denmark) and maintained under culture condition for 2 days at 37 °C in 5% humidified CO_2.

Proliferation Assay of MSCs on DTOPV Film Substrates. Two DTOPV films were prepared on glass substrates (5 cm × 5.5 cm) by spin coating. One of the films was exposed to UV with energy dose of 23.4 J/cm^2 and the other film was not exposed to UV. And then PDMS mold (3 cm × 3.5 cm) was attached to the two DTOPV films to preserve same area. The prepared DTOPV film substrates were washed with α-MEM supplemented with 10% FBS, 100 U/mL penicillin and 100 ug/mL streptomycin. And then the DTOPV film substrates with PDMS wall were placed in 100 mm culture dish (Corning, USA). Cells (from passage 4) were harvested with 0.05% Trypsin/EDTA for 3−5 min at 37 °C, placed at 2,000 cells/cm^2 in unexposed DTOPV substrate and UV-exposed DTOPV substrate. Cells (from passage 4) were harvested also on a tissue culture polystyrene(TCPS) with PDMS mold (3 cm × 3.5

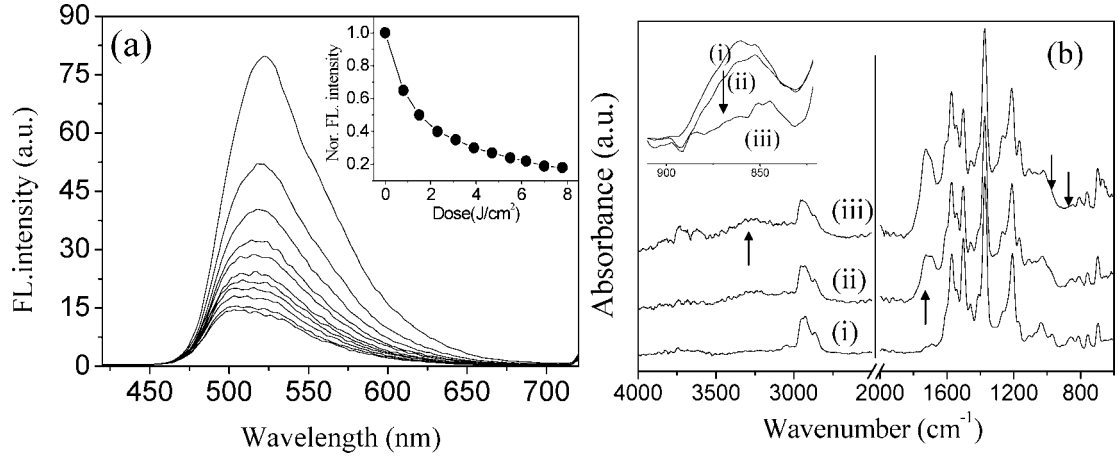

Figure 2. (a) Fluorescence spectra change of a DTOPV film at different irradiation time, from top to bottom, 0, 1, 2, 3, 4, 5, 6, 7, 8, 9, 10 min under air, inset- normalized FL intensity change of the film at 522 nm at different dose. (b) FT-IR spectra for a DTOPV film before irradiation (i) and after irradiation with a UV source for (ii) 15 min and (iii) 30 min (inset: magnification of the 920−820 cm^{-1} region).

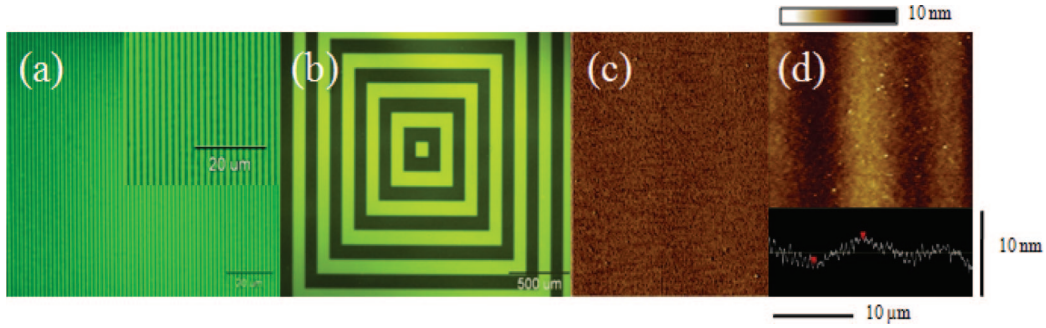

Figure 3. (a) and (b) Fluorescence microscope image of DTOPV film with 900 nm and 100 μm wide line patterns, respectively, prepared by photo-oxidation of DTTPV under UV irradiation. (c) EFM and (d) AFM image of the DTTPV film with 5 μm line patterns.

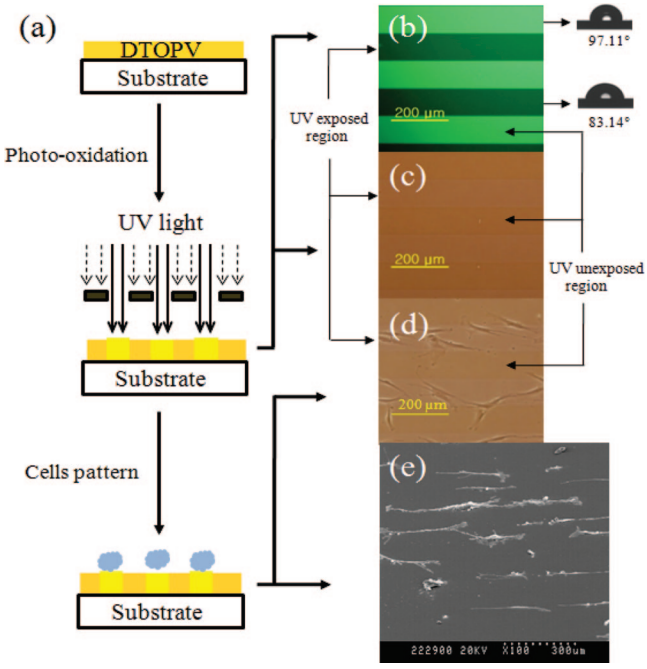

Figure 4. (a) Patterning procedure of a DTOPV coated substrate for cell pattern. (b) Fluorescent microscope image and water contact angle of the DTOPV pattern. (c) and (d) Optical microscope images of the patterned DTOPV surface (100 μm line width) before (c) and after (d) cells attachment. (e) Scanning electron microscope image of MSCs pattern attached to the patterned DTOPV surface (100 μm line width).

cm) as a reference experiment. Each well was dispensed with 3 mL α-MEM medium and changed once after 4 days. Cultures were maintained for 4 days and 6 days and then harvested for cell counting on day 4 and 6, respectively. This proliferation assay was examined at two different times. The growth rates for MSCs on the sample after 4 days and 6 days of culture were determined by counting the number of cells with a hemacytometer after tryphan blue staining in a counting chamber.

Interaction between MSCs and Several Proteins on DTOPV Pattern. Several proteins such as fibronectin, collagen, gelatin, albumin, and hIgG were investigated to explore the effect of proteins on cell pattern. Each protein solution, fibronectin in PBS, collagen type I in PBS, gelatin in PBS, albumin in PBS and hIgG in PBS, was mixed with serum-free α-MEM with 100 U/mL penicillin and 100 ug/mL streptomycin at final concentration of 10 ug/mL, respectively. The media including each protein was dispensed with cells at a concentration of 4000 cells/cm^2 on a DTOPV pattern substrate prepared with energy dose of 23.4 J/cm^2. Then the cells were incubated at 37 °C in 5% humidified CO_2 for 2 days. The number of cells attached per field, UV exposed and unexposed region on DTOPV pattern substrate, was determined from photographs taken of several samples with the Olympus inverted research microscope model IX71 at 100× magnification.

Results and Discussion

The Photo-Patterning of DTOPV Film by Photo-Oxidation. The polymer film surface used for the photopatterning experiments was a diphenylamino-s-triazine bridged *p*-phenylene vinylene (DTOPV) polymer (Figure 1) synthesized using the Wittig polycondensation method.[12,13] A solution of the polymer (1 wt %) in chloroform was spin-coated to afford a polymer film of 140 nm in thickness after solvent removal. The thin film of DTOPV showed an emission band maximized at 522 nm (Figure 2a), and 50% of the emission was extinguished when the film was exposed to a UV source for 2 min under ambient conditions. Figure 2a-inset shows fluorescence quenching under ambient conditions at various light doses. The fluorescence quenching originated from the photo-oxidation of the vinylene bond to give carbonyl products.[14] Indeed, the FT-IR spectrum of the DTOPV film in Figure 2b shows that the carbonyl peak (C═O stretching) at 1745 cm^{-1} was increased; at the same time, the vinylene peaks at 965 cm^{-1} (trans) and 855 cm^{-1} (cis)[14] were notably decreased after UV exposure. The integrated area of the absorbance at the 855 cm^{-1} band was decreased to 50% within 30 min. of UV exposure (Figure 2b, inset). Furthermore a broadband centered at ~ 3300 cm^{-1} was appeared indicating the formation of carboxylic acid (CO_2H) group. This result strongly indicates that the vinylene group in the DTOPV backbone structure was broken to give carbonyl compounds by the photo-oxidation, as described in Figure 1.[15]

Formation of CO_2H group could affect the surface charge. In order to examine electrostatic change of the surface, DTOPV was treated with crystal violet lactone, following the method reported in the literature.[16] When the UV exposed film was stained with crystal violet lactone, the intensity of the CO_2H band was decreased while those of the asymmetric and symmetric carboxylate vibration at 1572 cm^{-1} and 1375 cm^{-1} were significantly increased (Supporting Information, SFigure 1). The area intensity of those carboxylate vibration of the UV exposed part was ~10% higher than that of the UV unexposed sample. This indicates that the UV exposed film has negative character, due to the photogenerated CO_2H group, which allows preferential interaction of the surface with CVL.[17]

The photo-oxidation of DTOPV led to fluorescent pattern formation in the polymeric thin film. When the DTOPV thin film on a slide glass was exposed to a UV source through a photomask for 5 min, a clear fluorescent pattern was formed with line widths greater than 900 nm, depending on the line widths of the photomask (Figure 3, parts a and b).

Surface Properties of the DTOPV Pattern. Parts c and d of Figure 3 show electrostatic force microscopy (EFM) and atomic force microscopy (AFM) images of a 5 μm wide line pattern, respectively, prepared by photo-oxidation of the DTOPV film

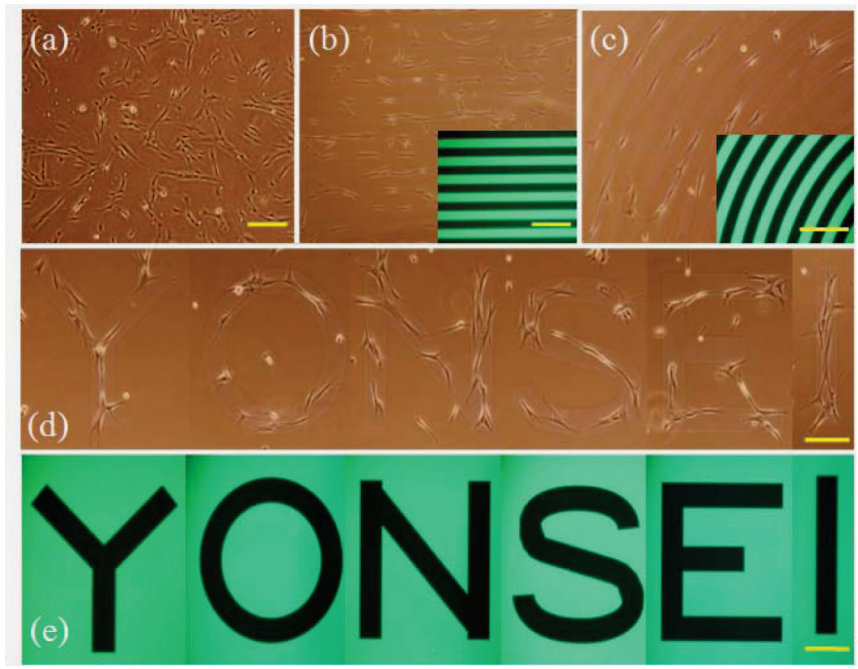

Figure 5. Optical microscope images of MSCs cultured on (a) tissue-culture polystyrene, (b) 50 μm-wide line pattern of DTOPV film, (c) 50 μm-wide curved line pattern of DTOPV film, (d) 100 μm-wide "YONSEI" letter pattern with MSCs on DTOPV film, and (e) fluorescent microscope image of the same "YONSEI" letter pattern with cells. Fluorescent pattern images are inserted in parts b and c. Scale bar = 200 μm.

under UV irradiation. The AFM image indicates that the surface of the DTOPV pattern was very smooth and uniform for both the UV-exposed and unexposed regions, with mean roughness (R_m) of 0.43 and 0.42 nm, respectively.

The depth decrease of the UV-exposed area of the film after UV irradiation, as determined by AFM, was very small, typically 1.1 and 2.8 nm for high doses of 23.4 and 46.8 J/cm^2, respectively. As the change in depth was smaller than 10 nm, and the mean roughness (R_m) change of the DTOPV film is negligible upon UV exposure, the topography and roughness effect on the attachments of cells or proteins on the DTOPV surface are negligible.[18,19]

We did the EFM experiment to see a difference in electrical conductivity change[20] on UV exposed vs non exposed region. Compared with the clear pattern shown in the AFM image in Figure 3d for the 5 μm wide line pattern, an EFM image for the pattern showed no detectable patterns or angle differences between the UV-exposed and unexposed areas, indicating that electrical conductivity change between the UV-exposed and unexposed regions is negligible [Figure 3c]. Although the π-electron delocalization of the *p*-phenylene unit would be partially reduced upon photo-oxidation, the conductivity change could not be detected through EFM image, possibly due to the high resistivity of the triazine bridging unit in DTOPV.

As described in Figure 1, DTOPV undergoes photo-oxidation to produce carbonyl derivatives that are more hydrophilic than the vinylene unit. In addition the surface charge could be more negative after photo-oxidation as described above in CVL staining test. Surface wettability changes of the DTOPV by UV irradiation were investigated by a contact angle study. The water contact angles of the film were found to gradually decrease from 97.1° (±0.05) to 92.2°, 91.1°, 90.8°, and 83.1° as the DTOPV film was exposed to UV for 0 to 15, 30, 45, and 60 min, respectively. The photo-oxidation of DTOPV dramatically altered surface properties of the film and boosted film wettability to hydrophilic and film charge to more negative, to alter cell attachment, patterning, alignment, and proliferation, as described below.

The biocompatibility of the DTOPV film was confirmed from a cell apoptosis experiment quantified using 7-aminoactinomycin D (7-AAD).[21,22] The proportion of dead MSCs on the standard tissue-culture polystyrene (TCPS) dish was determined as 3%; the proportions of dead MSCs on the UV-exposed and unexposed DTOPV films were 3% and 6%, respectively. This result demonstrates that the biocompatibility of the UV-exposed DTOPV is similar to the standard TCPS but much higher than the unexposed DTOPV.

Control of MSCs Adhesion and Proliferation Using DTOPV Film. Figure 4a shows the fabrication procedure of the DTOPV patterned substrate for the patterning of MSCs. This simple cell patterning method does not require labor-intensive preparation or careful control for cell patterning.[23] Parts b and c of Figure 4 show fluorescence microscopy and optical images of a 100 μm line pattern, respectively, confirming the uniform pattern formation on the DTOPV film by UV exposure. The contact angle of the UV-exposed area was smaller than that of the unexposed area, as shown in the photographs of the water droplet in Figure 4b.

For cell patterning studies, MSCs were seeded onto the patterned substrate in a culture medium and allowed to attach for overnight. The MSCs were preferentially adhered to and spread on the UV-exposed regions of the 100 μm wide line pattern and were prevented from extending onto the surrounding unexposed region [Figure 4d]. Furthermore, the cells were aligned in the direction of the line pattern (UV-exposed region). An SEM image [Figure 4e] shows an organized cell line formed on the patterned film arising from selective attachment of the cells to these UV-exposed lines. This resulted in the development of regular arrays of individual adherent cells that were aligned in the direction of the polymer line patterns.

Compared with the typical randomly attached spindle-shaped colonies on the TCPS [Figure 5a], the selective attachment and alignment of MSCs along the defined shape and pattern of the UV-exposed DTOPV film are clearly shown in Figure 5b−d. Surprisingly, MSCs align along curved and circular line patterns, Furthermore they aligned as a bending structure when the polymer pattern was a bent structure. This cell adherence and alignment properties according to the polymer patterns generated successfully the letter pattern of "YONSEI" with MSCs, where

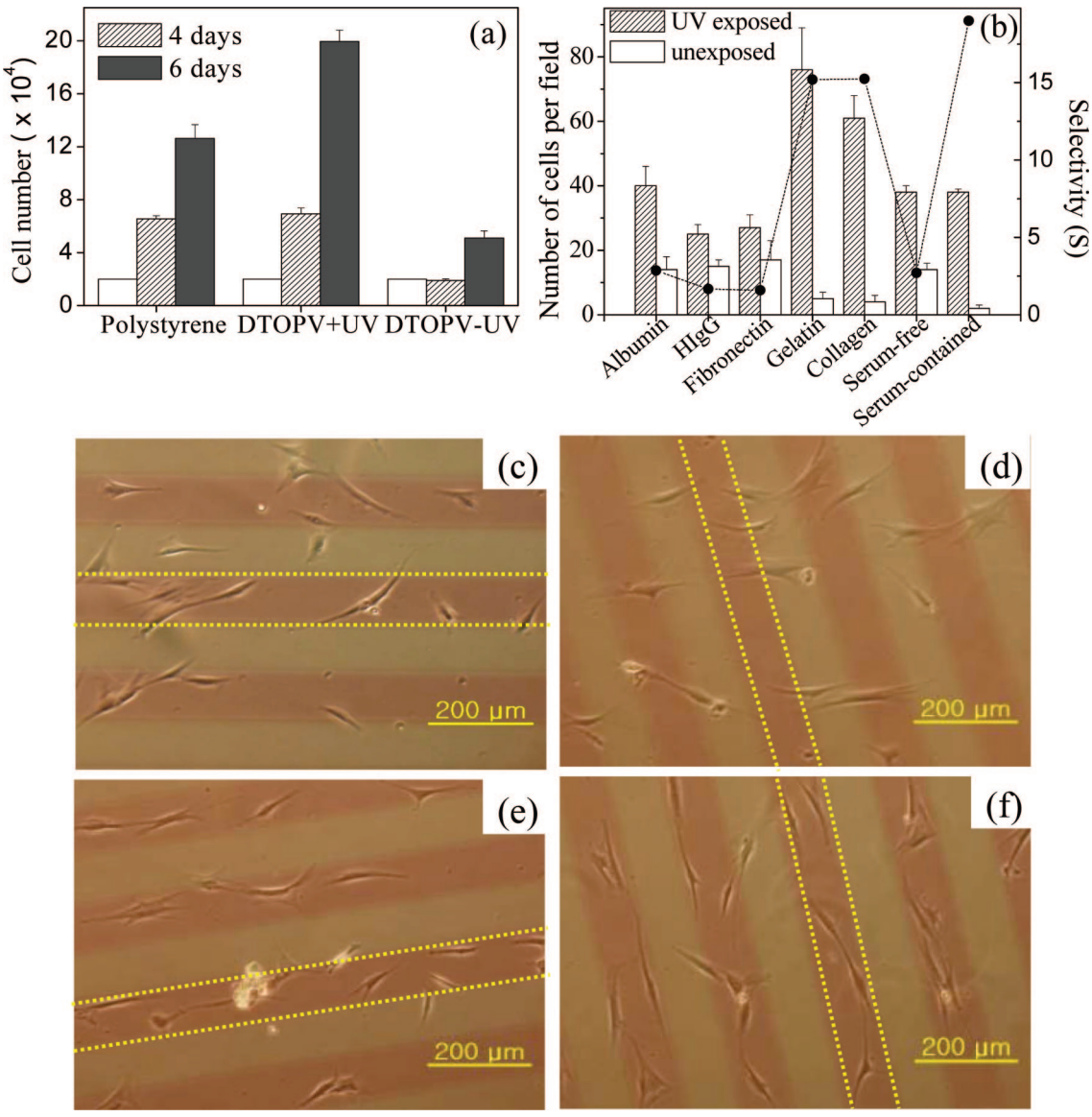

Figure 6. (a) Proliferation rate of MSCs cultured on TCPS as a reference, UV exposed DTOPV film (DTOPV+UV), and unexposed DTOPV film (DTOPV−UV) in serum contained culture medium for 4 and 6 day. MSCs were placed at a density of 2×10^3 cells/cm^2 at first (white box). (b) Number of cells per field attached to both UV exposed (shaded) and unexposed region (blank) of the DTOPV film in the presence of different proteins. (c−f) Optical microscopic images of MSCs cultured on the patterned DTOPV film (100 μm line width) in serum free medium in the presence of (c) no protein, (d) fibronectin, (e) collagen, and (f) gelatin. The images were obtained under the illumination of blue light. Scale bar = 200 μm.

line width of the pattern was 100 μm wide. However, these clear MSCs patterns started to collapse after 4 days of culture when MSCs were cultured on DOTPV pattern for a long time.

Importantly, the patterning of MSCs was dependent on the width of the line patterns. Thus, the cells were successfully adhered and aligned in the direction of the photopatterned DTOPV films when the width of the line patterns was 100 and 50 μm. However, for the narrower 20 μm wide line patterns, the MSCs were only randomly adhered to the pattern, possibly due to the size of the MSCs being larger than 20 μm.

Selective attachment of the MSCs on a hydrophilic surface has been reported previously.[24,25] Therefore, the patterning and alignment of MSCs on the DTOPV pattern could be explained similarly. As discussed above the UV-exposed region, where DTOPV undergoes photo-oxidation, contains carbonyl group at the polymer chain and thus the hydrophilicity of surface is increased (see Figures 1 and 4). Furthermore the surface charge of the UV exposed DTOPV film becomes more negative than that of the unexposed film. Such a hydrophilic and negative surface of the DTOPV film allows favorable interactions with cells to adhere and align on it.

To examine the proliferation rate of MSCs, cells were cultured on three different substrates: (1) tissue-culture polystyrene as a reference (TCPS), (2) UV-exposed DTOPV film under ambient conditions (DTOPV+UV), and (3) unexposed DTOPV film (DTOPV−UV). Figure 6a shows the proliferation rate of MSCs cultured on different substrates. MSCs seeded at the density of 2.0×10^3 cells/cm^2 were increased to 6.6×10^3 cells/cm^2 and 1.3×10^4 cells/cm^2 (6.5 fold) after 4 days and 6 days of culture, respectively, on TCPS. The proliferation rate of MSCs cultured on DTOPV+UV was higher, and increased to10-fold (2.0×10^4 cells/cm^2) after 6 days. This result indicates that the proliferation rate on the UV-exposed DTOPV film is much higher than that on TCPS, encouraging the potential application of DTOPV as a cell proliferation substrate. The proliferation rate of MSCs cultured on DTOPV−UV was very low, reaching only 5.1×10^3 cells/cm^2 (2.5 fold) after 6 days of culture due to poor attachment and compatibility of the cells on the substrate.

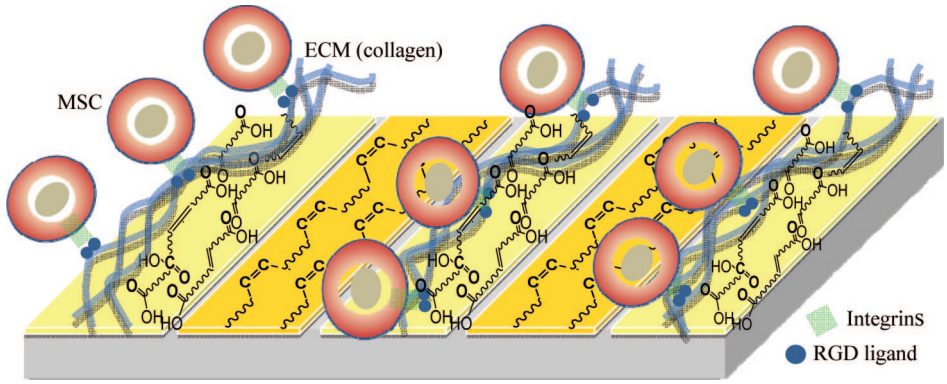

Figure 7. Model for cell adhesion and patterning on a photo-oxidized DTOPV surface.

The proliferation assay also indicated the high biocompatibility of the UV-exposed DTOPV film. These results indicate that not only the attachment but also the proliferation of MSCs was much more favorable on the UV-exposed film (DTOPV+UV) than that on the unexposed region (DTOPV−UV). After 6 days, MSCs cultured on DTOPV+UV surface showed confluence.

Optical microscopic images clearly shows cell location (for, e.g., Figure 5d) but not patterns. On the other hands, fluorescence microscope clearly shows patterns (for, e.g., Figure 5e) but not cells. Taking advantage of the fluorescence from the DTOPV pattern, the cell location and pattern images were easily detected simultaneously through the optical microscope under blue light illumination. As the unexposed region is emittive under the blue probe beam (460−480 nm), it appeared as brighter region, while the UV exposed region as darker. Thus pattern of the DTOPV was clearly seen as shown in Figure 6c−f. The pattern contrast was much higher as compared to the optical microscope images such as in Figure 4b or Figure 5d. Simultaneously cells on the darker lines were also clearly detected. Thus the pattern and the location of the cells could be easily identified by the optical microscope.

Effect of Extracellular Matrix on MSCs Pattern. Cell patterning was not observed in the serum-free condition, as shown in Figure 6c. Thus, it is considered that proteins present in extracellular matrix (ECM) influence the patterning of MSCs on photopatterned DTOPV films. For the investigation of the effect of proteins in ECM on the MSCs pattern, MSCs were seeded and cultured for 2 days on the patterned DTOPV films in the presence of proteins such as fibronectin, collagen, gelatin, albumin, and human serum immunoglobulin (hIgG) in serum-free α-MEM. Figure 6b shows number of cells attached to the DTOPV+UV. The cell attachment and alignment on the UV-exposed area were observed for the collagen- or gelatin-containing MSC cell mixtures. In the optical microscope with the blue probe on, cells were clearly detected on the DTOPV+UV lines as shown in Figure 6e,f. However, the cells were nonadherently spread over the UV-exposed and unexposed regions, without selectivity between the two areas, in other protein mixtures.

The selectivity (S) of the cells between the UV-exposed and unexposed regions is defined as the ratio of the numbers of cells on each region:

$$S = N_{UV}/N_{Dark} \tag{1}$$

where N_{UV} and N_{Dark} are the number of cells attached on the UV-exposed and unexposed regions of the DTOPV film, respectively. This selectivity indicates the selective attachments and patternability of the cells on the DTOPV patterns. As shown in Figure 6b, the S values for the collagen- and gelatin-containing MSC cell mixtures were comparable to the MSCs in serum. The number of cells attached to the DTOPV+UV were higher in the presence of collagen- and gelatin than that of the MSCs in serum. This result strongly support that collagen and gelatin in the serum strongly induce the selective attachments and patterning of MSCs on DTOPV+UV. In addition the S values for the collagen- and gelatin-containing cell mixtures were ∼9 times higher than that for fibronectin mixture. Osteoblastic cells (and various other cell types) *in vitro* have been shown to depend primarily on adsorbed proteins for initial adhesion and spreading, on surface including tissue culture polystyrene, titanium, stainless steel, and hydroxyapatite surface.[4] Thus, the ability of a surface to adsorb such proteins from serum determines their ability to support cell adhesion and spreading.[5]

The large difference in S values between the proteins above could be originated from the structure and functional group of proteins. As described above, the photo-oxidized surface of DTOPV is enriched with the hydrophilic carboxylic group to convert DTOPV more hydrophilic and more negative in electrostatic charge. Thus we ascribe the selective attachment and patterning of MSCs on the DTOPV+UV to the rapid adsorption of hydrophilic proteins from serum onto the presence of carboxylic group on the DTOPV+UV surface.

In particular, the fibronectin (Fn) containing MSC cell mixture showed not much preference on the UV-exposed over unexposed regions. It is widely accepted that ECM proteins present in serum adsorb onto the polymer scaffold first; then cells adhere to these serum-adsorbed proteins. The degree of proteins adsorption onto the polymer scaffold varies widely depending on the polymer substrate. Previous studies have demonstrated that the hydrophilicity of the material surface plays a critical role in cell adhesion and proliferation.[26] For example, collagen is primarily responsible for the adhesion of MSCs to poly(lactide-*co*-glycolide) (PLGA), while fibronectin plays lesser roles in MSC adhesion to it.[27] On the other hands, it has been reported that Fn affects adhesion of hMSCs as Fn coating can increase adhesion of hMSCs to some hydrophobic membranes (e.g., silicone membrane)[28] In our experiments, the cell attachment was poor on the patterned DTOPV in the presence of fibronectin compared to that contained collagen. Therefore, our result is consistent with the result from more polar surface such as PLGA.

Fibronectin exist as a dimer composed of two almost identical polypeptide subunits linked by a pair of C-terminal disulfide bonds.[29] Therefore fibronectin favors hydrophobic surface.[30] On the other hands, collagen and gelatin are known to be hydrophilic as they are consisting of polypeptide strands linked by numerous hydrogen bonds.[31] Thus the hydrophilic collagen and gelatin favorably interact with the photo-oxidized DTOPV surface, enabling these proteins to reside preferentially on the UV-exposed area. The primary interaction between cells and

adhesion proteins occurs via integrins (heterodimeric receptors in the cell membrane).[32] Therefore MSCs attach to and undergo cell culturing in the presence of hydrophilic proteins such as collagen and gelatin. A model for cell adhesion in the presence of collagen is conceptually drawn in Figure 7. Further studies on the photoirradiation process and the mechanism of MSCs patterning on DTOPV films are in progress, with the aim of optimizing and controlling cell patters on DTOPV.

Conclusion

The photoirradiation of DTOPV resulted in photo-oxidation of the vinylene units to change the surface wettability of the film to alter biocompatibility, cell attachment, patterning, alignment, and proliferation. The UV-exposed region showed a high proliferation rate for MSCs. The fluorescent pattern from the DTOPV film provided easy detection of the cell location and pattern images through a microscope with or without an excitation probe beam.These results open up potential application of photopatternable DTOPV films for cell patterning. Furthermore, this simple cell pattern method offers a new clue in attempts to isolate, immobilize, and control cells.

Acknowledgment. We acknowledge the financial support of Seoul R&BD Program (10816), and the Korea Science and Engineering Foundation (KOSEF) grant funded by the Korea government (MEST) (No. R11-2007-050-01001-0).

Supporting Information Available: Figure showing FT-IR spectra of the DTOPV film. This material is available free of charge via the Internet at http://pubs.acs.org.

References and Notes

(1) Molly, M. S.; Julian, H. G. *Science* **2005**, *310*, 1135–1138.
(2) Singhvi, R.; Kumar, A.; Lopez, G. P.; Stephanopoulos, G. N.; Wang, D. I. C.; Whitesides, G. M.; Ingber, D. E. *Science* **1994**, *264*, 696–698.
(3) (a) Mrksich, M.; Chen, C. S.; Xia, Y.; Dike, L. E.; Ingber, D. E.; Whitesides, G. M. *Proc. Natl. Acad. Sci. U.S.A.* **1996**, *93*, 10775–10778. (b) Ostuni, E.; Chapman, R. G.; Liang, M. N.; Meluleni, G.; Pier, G.; Ingber, D. E.; Whitesides, G. M. *Langmuir* **2001**, *17*, 6336–6343. (c) Yousaf, M. N.; Houseman, B. T.; Mrksich, M. *Proc. Natl. Acad. Sci. U.S.A.* **2001**, *98*, 5992–5996.
(4) (a) Steele, J. G.; McFarland, C.; Dalton, B. A.; Johnson, G.; Evans, M. D.; Howlett, C. R.; Underwood, P. A. *J. Biomater. Sci. Polym. Ed.* **1993**, *5*, 245–257. (b) Howlett, C. R.; Evans, M. D.; Walsh, W. R.; Johnson, G.; Steele, J. G. *Biomaterials* **1994**, *15*, 213–222.
(5) (a) Kilpadi, K. L.; Chang, P. L.; Bellis, S. L. *J. Biomed. Mater. Res.* **2001**, *57*, 258–267. (b) Steele, J. G.; Dalton, B. A.; Johnson, G.; Underwood, P. A. *J. Biomed. Mater. Res.* **1993**, *27*, 927–940.
(6) (a) Guo, L.; Kawazoe, N.; Fan, Y.; Ito, Y.; Tanaka, J.; Tateishi, T.; Zhang, X.; Chen, G. *Biomaterials* **2008**, *29*, 23–32. (b) Kim, S.; Rha, H.; Surendran, S.; Han, C.; Lee, S.; Choi, H.; Choi, Y.; Lee, K.; Rhie, J.; Ahn, S. *Macromol. Res.* **2006**, *14*, 565–572.
(7) Zhang, S.; Lin, Y.; Altman, M.; Lässle, M.; Nugent, Helen; Frankel, F.; Lauffenburger, D. A.; Whitesides, G. M.; Rich, A.*Biomaterials* **1999**, *20*, 1213–1220.
(8) Krol, S.; Nolte, M.; Diaspro, A.; Mazza, D.; Magrassi, R.; Gliozzi, A.; Fery, A. *Langmuir* **2005**, *21*, 705–709.
(9) Narita, T.; Hirai, A.; Xu, J.; Gong, J. P.; Osada, Y. *Biomacromolecules* **2000**, *1*, 162–167.
(10) Uttayarat, P.; Chen, M.; Li, M.; Allen, F. D.; Composto, R. J.; Lelkes, P. I. *Am. J. Physiol. Heart Circ. Physiol.* **2008**, *294*, H1027−H1035.
(11) (a) Ruiz, A.; Buzanska, L.; Gilliland, D.; Rauscher, H.; Sirghi, L.; Sobanski, T.; Zychowicz, M.; Ceriotti, L.; Bretagnol, F.; Coecke, S.; Colpo, P.; Rossi, F. *Biomaterials* **2008**, *29*, 4766–4774. (b) Tsuji, H.; Sommani, P.; Hattori, M.; Yamada, T.; Sato, H.; Gotoh, Y.; Ishikawa, J. *Nucl. Instrum. Methods Phys. Res. B* **2008**, *266*, 3067–3070. (c) Luo, W.; Jones, S. R.; Yousaf, M. N. *Langmuir* **2008**, *24*, 12129–12133.
(12) Yoo, J.; Kwon, T.; Sarwade, B.; Kim, Y.; Kim, E. *Appl. Phys. Lett.* **2007**, *91*, 241107–241109.
(13) (a) Yoo, J.; Jadhav, P.; Kim, E. *Mol. Cryst. Liq. Cryst.* **2008**, *491*, 114–121. (b) Kwon, T.; Sarwade, B.; Kim, Y.; Yoo, J.; Kim, E. *Mol. Cryst. Liq. Cryst.* **2008**, *486*, 101–109. (c) Cho, H.; Kim, E. *Macromolecules* **2002**, *35*, 8684–8687.
(14) (a) DeAro, J. A.; Gupta, R.; Heeger, A. J.; Buratto, S. K. *Synth. Met.* **1999**, *102*, 865–868. (b) Kim, Y.; Yun, C.; Jadhav, P.; You, J.; Kim, E. *Curr. Appl. Phys.*, in press.
(15) Rothberg, L. J.; Yan, M.; Papadimitrakopoulos, F.; Galvin, M. E.; Kwock, E. W.; Miller, T. M. *Synth. Met.* **1996**, *80*, 41–58.
(16) Douglas, C.; MacLaren, D. C.; White, M. A. *J. Mater. Chem.* **2003**, *13*, 1695–1700.
(17) (a) Mahoudas, N. *J. Theor. Biol.* **1975**, *49*, 417–424. (b) Lackie, A. M. *J. Cell Sci.* **1983**, *63*, 181–190.
(18) Dalby, M. J.; Riehle, M. O.; Sutherland, D. S.; Agheli, H.; Curtis, A. S. G. *J. Biomed. Mater. Res. Part A* **2004**, *69A*, 314–322.
(19) (a) Dalby, M. J.; McCloy, D.; Robertson, M.; Agheli, H.; Sutherland, D.; Affrossman, S.; Oreffo, R. O. C. *Biomaterials* **2006**, *27*, 2980–2987. (b) Dalby, M. J.; Riehle, M. O.; Johnstone, H. J. H.; Affrossman, S.; Curtis, A. S. G. *J. Biomed. Mater. Res. Part A* **2003**, *67A*, 1025–1032.
(20) (a) Schonenberger, C. *Phys. Rev. B* **1992**, *45*, 3861–3864. (b) Staii, C.; Johnson, A. T.; Pinto, N. J. *Nano Lett.* **2004**, *4*, 859–862.
(21) Philpott, N. J.; Turner, A. J. C.; Scopes, J.; Westby, M.; Marsh, J. C. W.; Gordon-Smith, E. C.; Dalgleish, G. A.; Gibson, F. M. *Blood* **1996**, *87*, 2244–2251.
(22) Wang, D.; Narang, A. S.; Kotb, M.; Gaber, A. O.; Miller, D. D.; Kim, S. W.; Mahato, R. I. *Biomacromolecules* **2002**, *3*, 1197–1207.
(23) Mitchell, S. A.; Davidson, M. R.; Emmison, N.; Bradley, R. H. *Surf. Sci.* **2004**, *561*, 110–120.
(24) Mitchell, S. A.; Davidson, M. R.; Bradley, R. H. *J. Colloid Interface Sci.* **2005**, *281*, 122–129.
(25) Sommani, P.; Tsuji, H.; Sato, H.; Hattori, M.; Yamada, T.; Gotoh, Y.; Ishikawa, J. *Trans. Mater. Res. Soc. Jpn.* **2007**, *32*, 921–924.
(26) Cheng, Z.; Teoh, S. H. *Biomaterials* **2004**, *25*, 1991–2001.
(27) Chastain, S. R.; Kundu, A. K.; Dhar, S.; Calvert, J. W.; Putnam, A. J. *J. Biomed. Mater. Res., Part A* **2006**, *78A*, 73–85.
(28) Song, G.; Ju, Y.; Soyama, H. *Mater. Sci. Eng.: C* **2008**, *28*, 1467–1471.
(29) Pankov, R.; Yamada, K. M. *J. Cell Sci.* **2002**, *115*, 3861–3863.
(30) Groth, T.; Altankov, G.; Klosz, K. *Biomaterials* **1994**, *15*, 423–428.
(31) (a) Rich, A.; Crick, F. H. C. *Nature* **1955**, *176*, 915–916. (b) Wei, H.; ZuWei, M.; Thomas, Y.; Wee, E. T.; Seeram, R. *Biomaterials* **2005**, *26*, 7606–7615.
(32) (a) Ruoslahti, E.; Pierschbacher, M. D. *Science* **1987**, *238*, 491–497. (b) Grzesik, W. J.; Robey, P. G. *J. Bone Miner. Res.* **1994**, *9*, 487–496.

MA802722Q